

**CORRELATED STABLE CALCIUM ISOTOPIC RATIO AND THULIUM ANOMALY IN REFRACTORY INCLUSIONS.** S. Huang<sup>1</sup>, J. Farkaš<sup>2</sup>, G. Yu<sup>1</sup> and S. B. Jacobsen<sup>1</sup>, <sup>1</sup>Department of Earth and Planetary Sciences, Harvard University (huang17@fas.harvard.edu), <sup>2</sup>Czech Geological Survey, Czech Republic.

**Introduction:** Refractory inclusions (RIs), including calcium-aluminum-rich inclusions (CAIs) and amoeboid olivine aggregates (AOAs), are the first condensates in the Solar System [1-3], and their origin is related to high-temperature condensation/evaporation processes in the solar nebula [4-7]. RIs show both mass dependent isotopic fractionations and non-mass dependent isotopic anomalies in many elements, such as O, Mg, Si, Ca, Mo, Ba, Nd and Sm. While the non-mass dependent isotopic anomalies in RIs reflect either incomplete isotopic mixing of isotopically anomalous pre-solar grains [e.g., 8-10], or excess of short-lived nuclides, such as <sup>26</sup>Al [e.g., 11], the mass-dependent isotopic fractionations are primarily generated by the condensation/evaporation processes that formed the RIs [e.g., 8, 10]. Condensation or evaporation is expected to generate coupled stable isotopic and elemental fractionations, controlled by their relative volatilities. However, such correlation has not yet been clearly established in RIs [8]. We are particularly interested in rare earth element (REE) abundances and Ca isotopes, because typically Ca and most REEs have similar condensation temperatures, and correlated fractionations in stable Ca isotopes and REE patterns are expected [8]. In this study, we report REE abundances, and mass dependent and non-mass dependent Ca isotopic compositions of six RIs extracted from the Allende CV3 carbonaceous chondrite.

**Analytical Procedures:** Small rock chips, several mg, of RIs (SJ101, SJ102 and SJ103), and several mg of powdered RIs (WFG, GFG and CGI) were dissolved in a 1:1 mixture of HF and HNO<sub>3</sub> acids. After full dissolution, three aliquots were taken for three types of measurements.

1. *Elemental Abundance Analysis:* Aliquots of solutions were diluted with 1.5% HNO<sub>3</sub> by a factor of 5000, and then analyzed for trace element abundances by traditional solution-ICP-MS technique using a GV Quadrupole ICP-MS at Harvard University. USGS standard samples, AGV-1, BCR-1 and BHVO-1, were used to construct the standard calibration curve. Analytical uncertainty of analyzed elements was estimated using multiple measurements of BHVO-2 solution analyzed as an unknown sample during the course of analysis, and it is better than 3% for all REEs.

2. *Non-Mass Dependent Ca Isotopic Analysis:* Ca was purified from the sample solution using a cation exchange technique [12]. Five μg of purified Ca was

loaded on a Re triple-filament assembly. The Ca isotopic abundances were measured using the Harvard IsoProbe-T TIMS with a two-sequence method. The first sequence collected masses <sup>40</sup>Ca, <sup>41</sup>K, <sup>42</sup>Ca, <sup>43</sup>Ca and <sup>44</sup>Ca, and the second <sup>44</sup>Ca and <sup>48</sup>Ca. The non-mass dependent isotopic compositions, expressed as ε<sup>4i</sup>Ca/<sup>44</sup>Ca relative to NIST SRM 915a, were measured using an online internal normalization to <sup>42</sup>Ca/<sup>44</sup>Ca of 0.31221 with exponential law, where ε<sup>4i</sup>Ca/<sup>44</sup>Ca = [(<sup>4i</sup>Ca/<sup>44</sup>Ca)<sub>sample</sub>/(<sup>4i</sup>Ca/<sup>44</sup>Ca)<sub>NIST915a</sub>-1]\*10<sup>4</sup>. Each sample was analyzed multiple times, and two standard error was used as the analytical uncertainty.

3. *Mass Dependent Ca Isotopic Analysis:* An aliquot of solution containing 20 μg Ca was mixed with a <sup>43</sup>Ca-<sup>48</sup>Ca double spike. After equilibration, Ca was separated from the sample-spike mixture, and the spiked Ca isotopic ratios were measured on TIMS following the same protocol described above for the non-mass dependent Ca isotopic analysis. The mass dependent Ca isotopic ratios, expressed as δ<sup>4i/4j</sup>Ca relative to NIST SRM 915a standard (δ<sup>4i/4j</sup>Ca = [(<sup>4i</sup>Ca/<sup>4j</sup>Ca)<sub>sample</sub>/(<sup>4i</sup>Ca/<sup>4j</sup>Ca)<sub>NIST915a</sub>]-1]\*1000), were determined by a <sup>43</sup>Ca-<sup>48</sup>Ca double spiking technique using an offline data reduction procedure with an exponential law [12]. Similarly, the analytical uncertainty (two standard error) was estimated based on multiple measurements. The detailed analytical procedure and the discussion of long-term external reproducibility can be found in Huang et al. [12].

**Results:** *REEs:* Two analyzed RIs show typical Group I (flat) REE patterns at ~20x chondritic level (Fig. 1). The other four have Group II REE patterns, depleted in ultra-refractory and volatile REEs [4, 5].

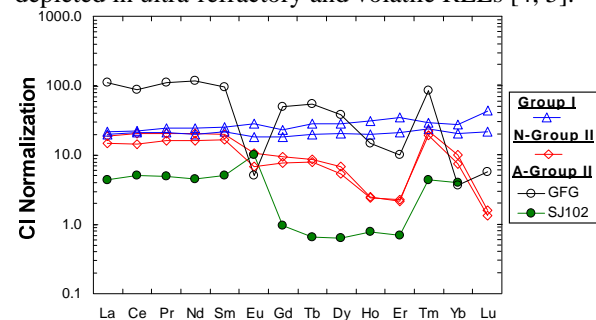


**Fig. 1** CI chondrite normalized REEs of RIs.

*Non-Mass Dependent Ca Isotopic Ratios:* ε<sup>40</sup>Ca/<sup>44</sup>Ca and ε<sup>43</sup>Ca/<sup>44</sup>Ca in six analyzed RIs range from -0.88 to 0.83, and from -0.5 to 1.2, respectively, which are indistinguishable from the analyzed terres-

trial standard NIST SRM 915a (Fig. 2a). In contrast, 5 out of 6 analyzed RIs have positive  $\epsilon^{48}\text{Ca}/^{44}\text{Ca}$  (2.5 to 8.2), clearly resolvable from the analyzed terrestrial standard NIST SRM 915a (Fig. 2a). This result is consistent with previous studies from [8, 9], but inconsistent with that by Simon et al. [13] who observed excess  $^{40}\text{Ca}$  in RIs. The small  $^{48}\text{Ca}$  excess in our analyzed RIs does not significantly affect our mass dependent Ca isotopic analysis, and its effect is smaller than our analytical uncertainty. This is because  $^{48}\text{Ca}$  is one of the spiked isotopes and the  $^{48}\text{Ca}$  budget in the spiked samples is dominated by the spike.

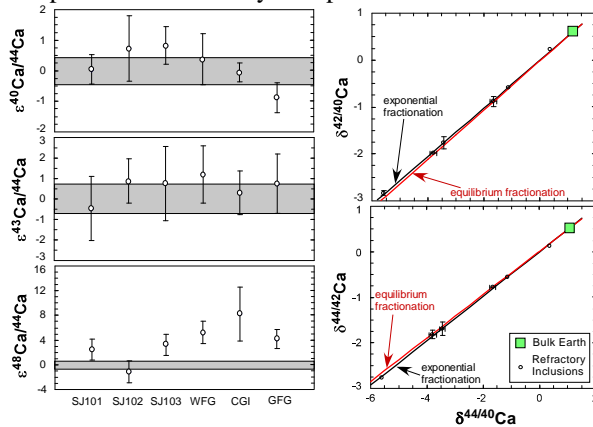


**Fig. 2a** (Left) Non-Mass Dependent and **b** (Right) Mass Dependent Ca Isotopic Ratios of RIs. The grey bars in panel **a** are defined by repeat measurements of NIST SRM 915a.

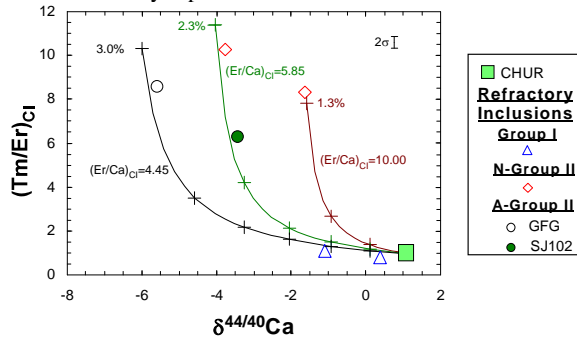


**Fig. 3**  $\delta^{44/40}\text{Ca}$  vs.  $(\text{Tm}/\text{Er})_{\text{CI}}$  in analyzed RIs. The analytical error on  $\delta^{44/40}\text{Ca}$  is smaller than the symbols, and the typical analytical error on Tm/Er is shown in the right-upper corner. The subscript CI denotes CI chondrite normalized value. A chondritic reservoir (CHUR) with Earth-like  $\delta^{44/40}\text{Ca}$  (1.05) [12] is shown for comparison. Three model trends showing the effects of segregation of a super-refractory evaporation residue from the CHUR prior to the condensation of RIs or their precursors are shown. This super-refractory evaporation residue is assumed to have HAL hibonate-like CaO content (9%) and  $\delta^{44/40}\text{Ca}$  (28, re-normalized to NIST 915a scale) [14, 15], and  $(\text{Tm}/\text{Er})_{\text{CI}}$  of 0.25, similar to those found in the super-refractory nodules [16, 17].  $(\text{Er}/\text{Ca})_{\text{CI}}$  in the super-refractory evaporation residue is varied from 4 to 10, which is shown next to the model trends. The maximum amounts of

the super-refractory evaporation residue segregated are shown near the ends of each model trends, and the tick marks represent 0.5% increments.

**Mass Dependent Ca Isotopic Ratios:** Stable Ca isotopic ratios ( $\delta^{44/40}\text{Ca}$ ,  $\delta^{44/42}\text{Ca}$  and  $\delta^{42/40}\text{Ca}$ ) of six analyzed RIs plot on the theoretically calculated exponential fractionation trends (Fig. 2b). Consequently, there are no detectable nucleosynthetic anomalies in  $^{40}\text{Ca}$ ,  $^{42}\text{Ca}$  or  $^{44}\text{Ca}$ , consistent with our non-mass dependent Ca isotopic measurements (Fig. 2a). The high precision of our mass dependent Ca isotopic data, and the large isotopic variations of the analyzed RIs allow us to distinguish between different fractionation laws: They fit exponential fractionation trends better than equilibrium fractionation trends. This is consistent with the results of the unspiked measurements (except for  $^{48}\text{Ca}$ ). Our analyzed RIs show coupled Ca isotopic and REE elemental fractionation. In detail, they form negative  $\delta^{44/40}\text{Ca}-(\text{Tm}/\text{Er})_{\text{CI}}$  trend, with  $R^2=0.60$  (Fig. 3).

**Discussion:** High  $(\text{Tm}/\text{Er})_{\text{CI}}$  is a typical feature of Group II REE patterns [4, 5]. It reflects a depletion of a super-refractory component enriched in heavy REEs, except for Tm. Such a super-refractory component would also be enriched in heavy Ca isotopes if it represents a high-temperature evaporation residue [14, 15]. Thus, the negative  $\delta^{44/40}\text{Ca}-(\text{Tm}/\text{Er})_{\text{CI}}$  trend in Fig. 3 can be explained by segregation of variable amounts (up to 3%) of a high-temperature, super-refractory evaporation residue, with high  $\delta^{44/40}\text{Ca}$ , from the solar nebula prior to the onset of condensation of RIs or their precursors [8].

**References:** [1] Grossman L. and Larimer J. W. (1974) *Rev. Geophys. Space Phys* 12, 71. [2] Gray, C. M. et al. (1973) *Icarus* 20, 213. [3] Amelin Y. et al. (2002) *Science* 297, 1678. [4] Ireland T. R. and Fegley B. JR. (2000) *Intern. Geol. Rev* 42, 865. [5] MacPherson G. J. (2004) In *Treatise on Geochemistry, No. 1* ed. Davis, A. M. pp 201-246. [6] Petaev M. I. and Jacobsen S. B. (2009) *GCA* 73, 5100. [7] Richter F. M. (2002) *GCA* 66, 521. [8] Niederer F. R. and Papanastassiou D. A. (1984) *GCA* 48, 1279. [9] Jungck M. H. A. et al. (1984) *GCA* 48, 2651. [10] Clayton R. N. et al. (1988) *Phil. Trans. R. Soc. Lond. A* 325, 483. [11] Lee T. et al. (1977) *ApJ* 211, L107. [12] Huang S. et al. (2010) *EPSL* 292, 337. [13] Simon J. I. et al. (2009) *ApJ*, 702, 707-715. [14] Lee T. et al. (1979) *ApJ* 228, L93. [15] Ireland T. R. et al. (1992) *GCA* 56, 2503. [16] El Goresy A. et al. (2002) *GCA* 66, 1459. [17] Hiyagon H. (2003) *LPS XXXIV*, #1552.